Acta Crystallographica Section F
Structural Biology and Crystallization Communications
ISSN 1744-3091

Cloning, expression, purification and preliminary X-ray diffraction studies of a novel AB_5 toxin

Natasha Ng,[a] Dene Littler,[a,b] Jérôme Le Nours,[a,b] Adrienne W. Paton,[c] James C. Paton,[c] Jamie Rossjohn[a,b,d] and Travis Beddoe[a]*

[a]Department of Biochemistry and Molecular Biology, Monash University, Clayton, Victoria, Australia, [b]Australian Research Council (ARC) Centre of Excellence in Structural and Functional Microbial Genomics, Monash University, Clayton, Victoria, Australia, [c]Research Centre for Infectious Diseases, School of Molecular and Biomedical Science, University of Adelaide, Adelaide, South Australia, Australia, and [d]Institute of Infection and Immunity, School of Medicine, Cardiff University, Heath Park, Cardiff CF14 4XN, Wales

Correspondence e-mail: travis.beddoe@monash.edu

Received 12 June 2013
Accepted 9 July 2013

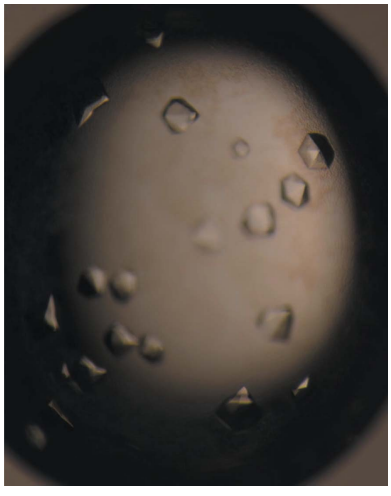

AB_5 toxins are key virulence factors found in a range of pathogenic bacteria. AB_5 toxins consist of two components: a pentameric B subunit that targets eukaryotic cells by binding to glycans located on the cell surface and a catalytic A subunit that disrupts host cellular function following internalization. To date, the A subunits of AB_5 toxins either have RNA-*N*-glycosidase, ADP-ribosyltransferase or serine protease activity. However, it has been suggested that a novel AB_5 toxin produced by clinical isolates of *Escherichia coli* and *Citrobacter freundii* has an A subunit with metalloproteinase activity. Here, the expression, purification and crystallization of this novel AB_5 toxin from *E. coli* (EcxAB) and the collection of X-ray data to 1.9 Å resolution are reported.

1. Introduction

AB_5 toxins are of immense importance because they are key virulence determinants of pathogenic bacteria, notably *Escherichia coli*, *Shigella dysenteriae* and *Vibrio cholerae*, which collectively cause massive global morbidity and mortality. These toxins comprise a catalytic A subunit linked to a pentameric B subunit. They exert their effects in a two-step process: the B subunit pentamer first binds to specific glycan receptors on the cell surface, triggering uptake and intracellular trafficking of the holotoxin; this is followed by inhibition or corruption of essential host functions mediated by the enzymatic activity of the A subunit (Beddoe *et al.*, 2010).

Until a decade ago, the enzymatic activities ascribed to these A subunits were either ADP-ribosyltransferase or RNA-*N*-glycosidase. However, a novel AB_5 toxin termed subtilase cytotoxin (SubAB) with a proteolytic A subunit has since been described (Paton *et al.*, 2004). The sole molecular target of SubAB was identified as the endoplasmic reticulum (ER) molecular chaperone BiP/GRP78, a master regulator of ER function, while its B subunit had unique specificity for a sugar acquired from dietary intake (Paton *et al.*, 2006; Byres *et al.*, 2008). Since the discovery of SubAB, the enzymatic activity of SubA has been exploited as a powerful cell-biological tool to probe the role of BiP in diverse cellular processes (Hu *et al.*, 2009; Eletto *et al.*, 2012; Schäuble *et al.*, 2012). Previous studies have also identified additional putative AB_5 toxin operons in *E. coli* and *Citrobacter freundii* diarrhoea isolates (designated *ecxAB* and *cfxAB*, respectively) by cross-reaction with antibodies to the B subunits of cholera toxin (CtxB) and heat-labile enterotoxin (LTB) (Karasawa *et al.*, 2002). The expressed B subunits of these novel toxins (EcxB and CfxB) are 87% identical to each other and 72–74% identical to both CtxB and LTB. The crystal structure of CfxB superimposes closely on CtxB, and CfxB bound glycans known to interact with CtxB and LTB (Jansson *et al.*, 2010). Interestingly, EcxA and CfxA both contain a sequence motif (HE*X*GH*XX*G*XX*H) that is characteristic of the active site of bacterial metalloproteinases (Bode *et al.*, 1999). However, it has not been shown that EcxA or CfxA can associate with their cognate B subunits.

To investigate whether EcxAB represents a novel AB_5 toxin, we have prepared and crystallized the EcxAB complex. Structural determination of EcxAB will provide valuable insight into the mechanistic function of this novel putative AB_5 toxin.

2. Materials and methods

2.1. Cloning

The cloning of the *ecxA* and *ecxB* genes into modified pBAD18 vector (Guzman *et al.*, 1995) was performed by chemical synthesis of both genes (GenScript, New Jersey, USA), replacing the native signal sequence with the pelB signal sequence and with the addition of restriction sites *Nde*I and *Xma*I and *Nco*I and *Xho*I flanking the *ecxA* and the *ecxB* open reading frames, respectively. The *ecxA* sequence encoding residues ^{22}ERTPN . . . SGGDL^{285} of the mature protein was directly cloned into pBAD-18 using *Nde*I and *Xma*I restriction sites, while the *ecxB* sequence encoding residues ^{22}ATPQN . . . IELSN^{125} of the mature protein was cloned into pET-23 (Novagen) *via Nco*I and *Xho*I sites, resulting in a protein with a C-terminal poly-His tag. To produce the co-expression vector for EcxAB, the ribosome binding site and *ecxB* were excised by restriction enzymes *Xba*I and *Hin*dIII and cloned downstream of *ecxA* (Fig. 1*a*). The clone obtained was confirmed by DNA sequencing.

2.2. Overexpression of recombinant protein

Recombinant protein expression of EcxAB was performed in *E. coli* strain BL21(DE3). A starter culture was grown overnight in LB medium containing ampicillin (100 µg ml^{-1}) at 310 K. The starter culture was used at a dilution of 1:100 to inoculate 800 ml fresh LB medium containing 100 µg ml^{-1} ampicillin and was grown at 310 K until the OD_{600} reached 0.6. Expression of EcxAB was induced with 0.2%(*w*/*v*) L-arabinose and the cells were allowed to grow for a further 4 h at 310 K. The cells were collected following centrifugation at 5000*g* for 20 min at 277 K and stored at 193 K.

2.3. Purification of recombinant protein

Cells were thawed and resuspended in Tris-buffered saline (TBS; 20 m*M* Tris pH 8, 150 m*M* NaCl) and lysed using a cell disruptor (Avestin) in the presence of 0.2 µ*M* phenylmethanesulfonylfluoride (PMSF). Cell debris was removed by centrifugation at 30 000*g* for 30 min at 277 K. All subsequent purification steps were performed at 293 K. High-speed supernatant was collected and loaded onto 5 ml nickel Sepharose beads (GE Healthcare) equilibrated in binding buffer (50 m*M* Tris–HCl pH 8.0, 500 m*M* NaCl, 60 m*M* imidazole). Unbound material was removed by washing with two column volumes of binding buffer. The protein was eluted using four column volumes of elution buffer (50 m*M* Tris–HCl pH 8.0, 500 m*M* NaCl, 1 *M* imidazole). Fractions containing EcxAB were pooled, buffer-exchanged into TBS and concentrated to 5 ml by low-speed centrifugation using a Vivaspin-2 50 000 Da molecular-weight cutoff (Sartorius Stedim Biotech). EcxAB was further purified by size-exclusion chromatography using an ÄKTA Basic Fast Protein Liquid Chromatography (FPLC) system with a Superdex S200 16/60 gel-filtration column (GE Healthcare Life Sciences) equilibrated in TBS. The molecular weight, purity and identity of the EcxAB preparation were confirmed by SDS–PAGE (Fig. 1*b*), Western blotting with anti-hexahistidine antibody (R&D systems) and N-terminal sequencing. The purified protein was concentrated to 5 mg ml^{-1} and stored at 277 K for use in crystallization trials. The concentration of EcxAB was determined spectrophotometrically (NanoDrop 1000, Thermo Scientific) at 280 nm and was calculated using an extinction coefficient of 81 430 M^{-1} cm^{-1}.

2.4. Crystallization

The initial crystallization experiments involved screening 192 conditions in commercially available kits from Hampton Research (Crystal Screen HT and PEG/Ion HT) using the CrystalMation integrated robotic workstation (Rigaku) and the sitting-drop vapour-diffusion technique. Initial crystals were obtained in condition E9 of the PEG/Ion HT screen [4%(*v*/*v*) Tacsimate pH 4, 12%(*w*/*v*) PEG 3350]. Optimization of the EcxAB crystallization conditions was performed by fine-screening the initial condition by varying the protein and precipitant concentrations using the hanging-drop method in 24-well Linbro plates (Hampton Research) with drops consisting of 1 µl protein solution and 1 µl precipitant solution and a

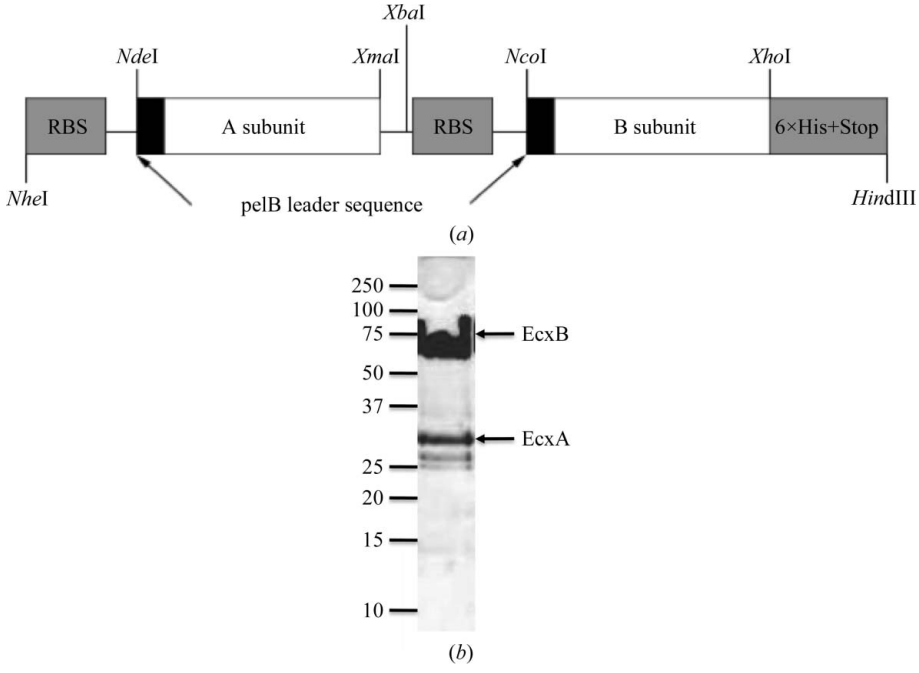

Figure 1
(*a*) Schematic of the co-expression vector for EcxAB. (*b*) 18% SDS–PAGE of purified non-boiled EcxAB. Molecular weights (in kDa) are indicated on the left.

reservoir volume of 500 µl. Crystals appeared in most conditions; however, the best crystals appeared after 1 d in 4%(*v*/*v*) Tacsimate pH 4.5, 10%(*w*/*v*) PEG 3350 (Fig. 2), which was found after several optimization plates.

2.5. X-ray data collection

For data collection, crystals were transferred to cryoprotectant solution consisting of 20%(*v*/*v*) glycerol, 4%(*v*/*v*) Tacsimate pH 4.5, 10%(*w*/*v*) PEG 3350 before cooling to 100 K in a stream of nitrogen gas. The majority of the crystals diffracted to better than 2.2 Å resolution (Fig. 3) and a complete data set was collected from a single crystal on the MX2 beamline at the Australian Synchrotron using an ADSC Quantum 315r CCD detector. The data were processed with *MOSFLM* (Leslie & Powell, 2007) and various programs from the *CCP*4 suite (Winn *et al.*, 2011). The final statistics for data collection and processing are summarized in Table 1.

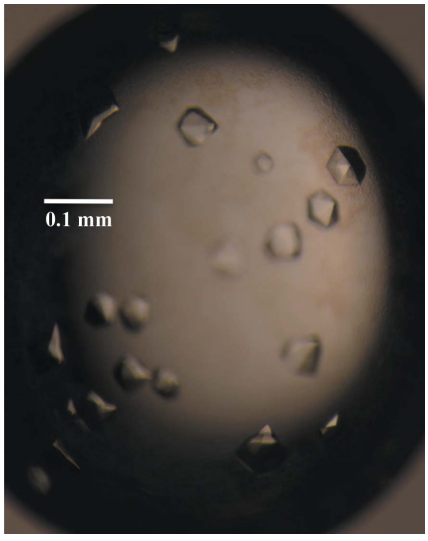

Figure 2
Diffraction-quality crystals of EcxAB.

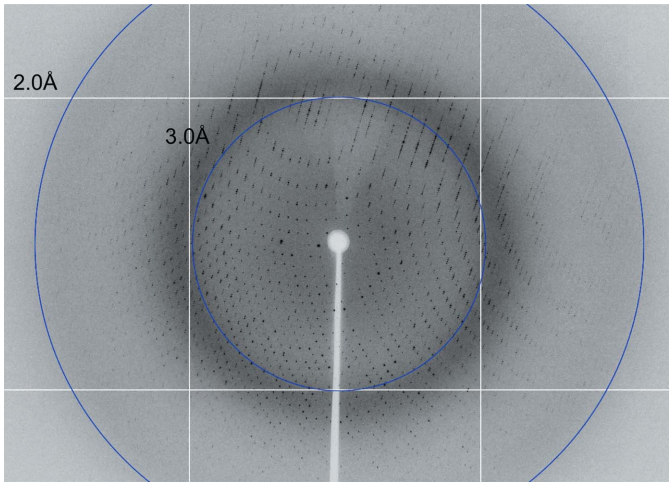

Figure 3
A diffraction pattern of an EcxAB crystal.

Table 1
Crystal and data-collection statistics for apo EcxAB.

Values in parentheses are for the outer shell.

Diffraction source	MX2, Australian Synchrotron
Detector	ADSC Quantum 315r CCD
Space group	$P6_522$
Temperature (K)	100
Unit-cell parameters (Å, °)	$a = b = 120.7$, $c = 274.3$, $\alpha = \beta = \gamma = 90.0$
Resolution range (Å)	39.5–1.80 (1.90–1.80)
Wavelength (Å)	0.9537
Total No. of reflections	109241
No. of unique reflections	15721
R_{merge}† (%)	7.2 (55.1)
Mean $I/\sigma(I)$‡	8.2 (1.4)
Completeness (%)	99.9 (100)

† $R_{merge} = \sum_{hkl}\sum_i |I_i(hkl) - \langle I(hkl)\rangle| / \sum_{hkl}\sum_i I_i(hkl)$, where $I_i(hkl)$ is the scaled intensity of the ith measurement and $\langle I(hkl)\rangle$ is the mean intensity for that reflection. ‡ I is the intergrated intensity and $\sigma(I)$ is the estimated standard deviation of that intensity.

3. Results and discussion

The *ecxA* and *ecxB* genes were successfully cloned, co-expressed, purified and crystallized using vapour-diffusion methods. The EcxAB complex was purified to homogeneity and the pentameric arrangement of EcxB was retained when the sample was not boiled before SDS–PAGE analysis (Fig. 1*b*). This is a hallmark of B-subunit pentamers (Lebens *et al.*, 1996). This expression and purification strategy routinely produced yields of 10 mg l^{-1}. Crystals of EcxAB were obtained in 4%(*v*/*v*) Tacsimate pH 4.5, 10%(*w*/*v*) PEG 3350 (Fig. 2) and a complete diffraction data set to 1.9 Å resolution was collected at 100 K. The preliminary crystallographic analysis indicated that the crystals belonged to space group $P6_522$, with unit-cell parameters $a = b = 120.7$, $c = 274.3$ Å, $\alpha = \beta = \gamma = 90.0°$. The data-collection and processing statistics are summarized in Table 1. Based on Matthews coefficient calculations, one EcxAB complex (~60% solvent content) could be accommodated in the asymmetric unit (Matthews, 1968). Structure determination by means of molecular replacement appears feasible as the known structure of *C. freundii* CfxB (PDB entry 2wv6; Jansson *et al.*, 2010) shares 87% sequence identity with EcxB. Structure verification and model rebuilding are currently in progress.

We thank the staff of the Australian Synchrotron and Monash Macromolecular Crystallization Facility for assistance with crystallization and X-ray data collection. The Australian Research Council and the National Health and Medical Research Council of Australia supported this work. TB is a Pfizer Australian Research Fellow, AWP is an Australian Research Council DORA Fellow, JCP is an NHMRC Senior Principal Research Fellow and JR is an NHMRC Australia Fellow.

References

Beddoe, T., Paton, A. W., Le Nours, J., Rossjohn, J. & Paton, J. C. (2010). *Trends Biochem. Sci.* **35**, 411–418.
Bode, W., Fernandez-Catalan, C., Tschesche, H., Grams, F., Nagase, H. & Maskos, K. (1999). *Cell. Mol. Life Sci.* **55**, 639–652.
Byres, E., Paton, A. W., Paton, J. C., Löfling, J. C., Smith, D. F., Wilce, M. C. J., Talbot, U. M., Chong, D. C., Yu, H., Huang, S., Chen, X., Varki, N. M., Varki, A., Rossjohn, J. & Beddoe, T. (2008). *Nature (London)*, **456**, 648–652.
Eletto, D., Maganty, A., Eletto, D., Dersh, D., Makarewich, C., Biswas, C., Paton, J. C., Paton, A. W., Doroudgar, S., Glembotski, C. C. & Argon, Y. (2012). *J. Cell Sci.* **125**, 4865–4875.
Guzman, L. M., Belin, D., Carson, M. J. & Beckwith, J. (1995). *J. Bacteriol.* **177**, 4121–4130.
Hu, C.-C. A., Dougan, S. K., Winter, S. V., Paton, A. W., Paton, J. C. & Ploegh, H. L. (2009). *J. Exp. Med.* **206**, 2429–2440.

Jansson, L., Angström, J., Lebens, M., Imberty, A., Varrot, A. & Teneberg, S. (2010). *Biochimie*, **92**, 482–490.
Karasawa, T., Ito, H., Tsukamoto, T., Yamasaki, S., Kurazono, H., Faruque, S. M., Nair, G. B., Nishibuchi, M. & Takeda, Y. (2002). *Infect. Immun.* **70**, 7153–7155.
Leslie, A. G. W. & Powell, H. R. (2007). *Evolving Methods for Macromolecular Crystallography*, edited by R. J. Read & J. L. Sussman, pp. 41–51. Dordrecht: Springer.
Lebens, M., Shahabi, V., Bäckström, M., Houze, T., Lindblad, N. & Holmgren, J. (1996). *Infect. Immun.* **64**, 2144–2150.
Matthews, B. W. (1968). *J. Mol. Biol.* **33**, 491–497.
Paton, A. W., Beddoe, T., Thorpe, C. M., Whisstock, J. C., Wilce, M. C. J., Rossjohn, J., Talbot, U. M. & Paton, J. C. (2006). *Nature (London)*, **443**, 548–552.
Paton, A. W., Srimanote, P., Talbot, U. M., Wang, H. & Paton, J. C. (2004). *J. Exp. Med.* **200**, 35–46.
Schäuble, N., Lang, S., Jung, M., Cappel, S., Schorr, S., Ulucan, Ö., Linxweiler, J., Dudek, J., Blum, R., Helms, V., Paton, A. W., Paton, J. C., Cavalié, A. & Zimmermann, R. (2012). *EMBO J.* **31**, 3282–3296.
Winn, M. D. *et al.* (2011). *Acta Cryst.* D**67**, 235–242.